

# Subsolidus Phase Relationships in the Systems $\text{Ln}_2\text{O}_3\text{--Si}_3\text{N}_4\text{--AlN--Al}_2\text{O}_3$ ( $\text{Ln} = \text{Nd}, \text{Sm}$ )

W. Y. Sun, D. S. Yan, L. Gao,

The State Key Lab on High Performance Ceramics and Superfine Microstructure, Shanghai Institute of Ceramics, Academia Sinica, Shanghai, People's Republic of China

H. Mandal, K. Liddell & D. P. Thompson

Wolfson Laboratory, Materials Division, Department of Mechanical, Materials & Manufacturing Engineering, University of Newcastle upon Tyne, UK

(Received 14 April 1994; revised version received 14 July 1994; accepted 1 August 1994)

## Abstract

*Subsolidus phase relationships in the systems  $\text{Ln--Si--Al--O--N}$  where  $\text{Ln} = \text{Nd}$  and  $\text{Sm}$  have been determined. Forty-four compatibility tetrahedra were established in the region  $\text{Ln}_2\text{O}_3\text{--Si}_3\text{N}_4\text{--AlN--Al}_2\text{O}_3$ . Within this region,  $\text{LnAlO}_3$  and  $M'$ -phase ( $\text{Ln}_2\text{Si}_{3-x}\text{Al}_x\text{O}_{3+x}\text{N}_{4-x}$ ) are the only two important compounds which have tie lines joined to  $\beta$ -sialon and AlN polytypoid phases.  $\alpha$ -Sialon coexists with the  $M'$  phase.*

## 1 Introduction

It is well known that metal oxides are necessary for the densification of silicon nitride ceramics. During sintering, the metal oxide additives and silicon nitride (which unavoidably contains a small amount of silica as an impurity), form an eutectic melt which aids densification. The liquid composition affects the resulting microstructure and hence the properties of the final ceramics; it also determines the nature of grain-boundary crystalline phases after heat-treatment.

The importance of using rare earth oxides for the densification of silicon nitride ceramics has been recognized during recent years. Not only are they very effective for densification, either singly, or in combination with yttria, but also they can be accommodated in the  $\alpha$ -sialon lattice, thus providing an opportunity for decreasing the transient liquid phase content after sintering, and hence reducing the amount of residual grain boundary glass. Therefore, phase relationships in  $\text{Ln--Si--Al--O--N}$  systems are of particular interest. The determination of a whole system, represents a very large

amount of work and most previous studies have been restricted to the sub-systems  $\text{Ln--Si--O--N}$ ,<sup>1</sup>  $\text{Ln--Al--O--N}$  ( $\text{Ln} = \text{Ce}, \text{Pr}, \text{Nd}$  and  $\text{Sm}$ )<sup>2</sup> and some planes involving  $\alpha$ - and  $\beta$ -sialon.<sup>3,4</sup> In oxygen-rich compositions, there exist two five-component phases,<sup>5-7</sup> U-phase ( $\text{Ln}_3\text{Si}_{3-x}\text{Al}_{3+x}\text{O}_{12+x}\text{N}_{2-x}$ ) and W-phase ( $\text{Ln}_4\text{Si}_9\text{Al}_5\text{O}_{30}\text{N}$ ), which have no corresponding counterparts in the  $\text{Y--Si--Al--O--N}$  system. In the  $\text{Ln}_2\text{O}_3\text{--Si}_3\text{N}_4\text{--AlN--Al}_2\text{O}_3$  sub-system where  $\text{Ln} = \text{Sm}, \text{Nd}$ , four compounds: Ln-melilite,  $\text{LnAlO}_3$ ,  $\text{Ln}_2\text{AlO}_3\text{N}$  and MP ( $\text{LnAl}_{12}\text{O}_{18}\text{N}$ ) have been identified (Fig. 1). The Ln-melilite phase extends into a five-component system, with Si and N being substituted by Al and O to form a solid solution,  $M'$ , with a range of homogeneity from  $x = 0$  to 1 in the formula  $\text{Ln}_2\text{Si}_{3-x}\text{Al}_x\text{O}_{3+x}\text{N}_{4-x}$ .<sup>8,9</sup> Work at Shanghai<sup>2</sup> on  $\text{Ln--Al--O--N}$  systems has shown that the nitrogen-containing magnetoplumbite phase of formula  $\text{LnAl}_{12}\text{O}_{18}\text{N}$  is unstable in the pure oxide system.

The purpose of the present work is to complete the study of phase relationships in the region of the  $\text{Ln--Si--Al--O--N}$  systems defined by the four end-members  $\text{Si}_3\text{N}_4$ , AlN,  $\text{Al}_2\text{O}_3$  and  $\text{Ln}_2\text{O}_3$  ( $\text{Ln} = \text{Nd}, \text{Sm}$ ). This region includes the phases  $\alpha$ -sialon,  $\beta$ -sialon and AlN polytypoids, and covers the range of compositions used for the design and processing of commercial multi-phase sialon ceramics.

## 2 Experimental Procedure

The present paper is the result of two work programmes carried out separately at Shanghai Institute of Ceramics and the University of

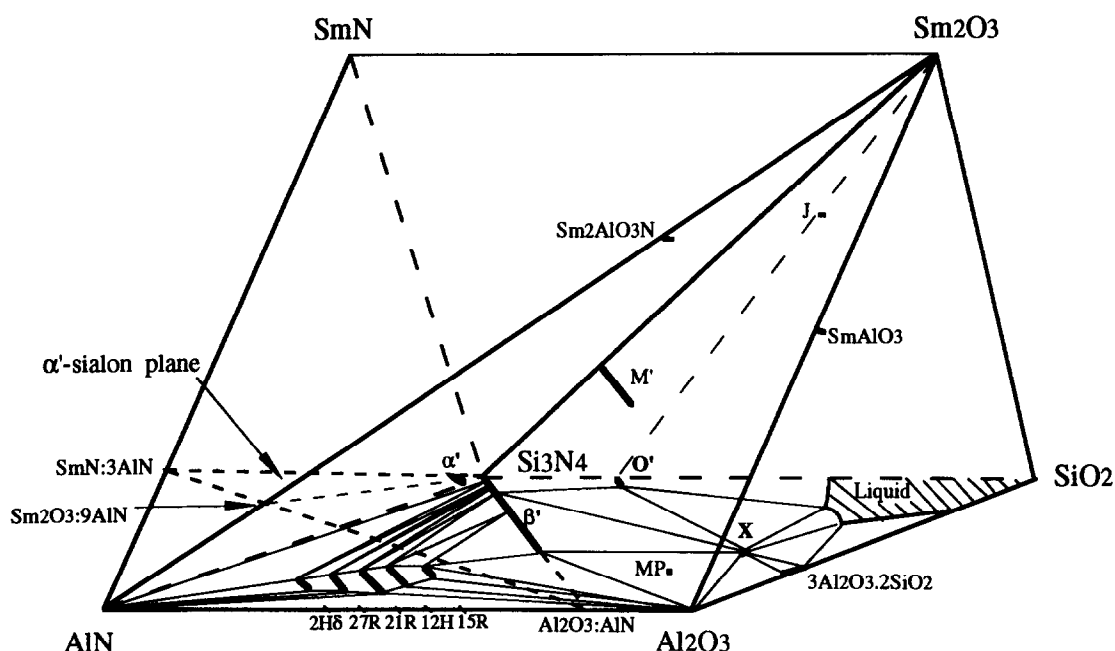


Fig. 1. Representation of Sm(Nd)-SiAlON system showing phases occurring in the region bounded by  $\text{Si}_3\text{N}_4$ ,  $\text{Sm}(\text{Nd})_2\text{O}_3$ ,  $\text{Al}_2\text{O}_3$  and  $\text{AlN}$ , and Si-Al-O-N behaviour diagram at  $1700^\circ\text{C}$ .

Newcastle. The symbols '#' and '\*' are used to represent the experiments carried out at Shanghai and Newcastle, respectively. The starting powders used were  $\alpha$ - $\text{Si}_3\text{N}_4$  (Starck H1# and Starck LC10\*),  $\text{AlN}$  (supplied by Zhuzhou Institute of Hard

Metal Alloys#, containing 1.2% oxygen and Starck Grade B\*),  $\text{Al}_2\text{O}_3$  (99.99%, produced by decomposing ammonium alum# and Alcoa A17\*),  $\text{Nd}_2\text{O}_3$  (99.9%, Yaolung Chemical Works, China# and 99.9%, Aldrick Chemical Co. Ltd\*) and  $\text{Sm}_2\text{O}_3$

Table 1. Compositions studied in the system  $\text{Si}_3\text{N}_4$ - $\text{AlN}$ - $\text{Al}_2\text{O}_3$ - $\text{Nd}_2\text{O}_3$

No.	$\text{Si}_3\text{N}_4$	Compositions (wt%)			Firing ( $^\circ\text{C}$ -h)	Phases present	Heat treat.	Phases present
		$\text{AlN}$	$\text{Al}_2\text{O}_3$	$\text{Nd}_2\text{O}_3$				
1#	70.75	7.08	8.00	14.17	HP1750-1	$\beta_6\text{s}$ ; M'm		
2#	57.19	10.58	18.08	14.16	HP1750-1	$\beta_{15}\text{s}$ ; 12Hw	1350-24^ 1550-5	$\beta_{15}\text{s}$ ; As; 12Hvw $\beta_{15}\text{s}$ ; 12Hw
3#	55.22	17.25	0.84	26.69	HP1750-1	M'vs; $\alpha'$ s; 21Rvw		
4#	53.26	17.99	2.08	26.67	HP1750-1	M'vs; $\alpha'$ s; 21Rw; $\beta'$ vw		
5#	25.95	3.79	23.58	46.68	1500-2	Avs; $\beta'$ w		
6#	19.75	16.90	27.55	35.65	1550-2	As; 15Rm		
7#	19.61	3.64	6.19	70.56	1700-2	M'vs; Jvw		
8#	14.45	35.30	14.05	35.12	1750-2	M'vs; 21Rm; $\alpha'$ w		
9#	11.77	6.52	—	81.71	1600-2	Jvs; M's		
10#	11.77	—	13.95	74.28	1550-2	As; M's; Hw		
11#	11.77	33.26	—	54.97	1700-2	M'vs; AlNw		
12#	10.57	37.51	43.09	8.74	1750-2	15Rs; MPm; $\text{Al}_2\text{O}_3$ vw		
13#	9.77	5.71	14.20	70.31	1550-2	Avs; M's; Hvw		
14#	9.17	41.07	40.95	8.74	1700-2	MPs; 21Rs		
15#	6.10	50.00	—	43.90	1650-2	M's; AlNs; Jm		
16#	4.88	—	13.95	81.17	1600-2	Avs; M's; Jw; Hw		
17#	4.88	6.52	—	88.60	1600-2	Ns; Js; $\text{Nd}_2\text{O}_3\text{s}$		
18#	80.00	—	4.65	15.35	1700-1	$\beta\text{vs}$ ; aw; M'vw	1350-24 1550-5^	$\beta\text{s}$ ; Hm; $\alpha\text{vw}$ $\beta\text{vs}$ ; M's; $\alpha\text{vw}$
19*	75.91	1.09	1.85	21.15	1800-1	$\beta\text{vs}$ ; M'w	1550-5	M'vs; $\beta\text{s}$
20*	59.73	16.78	1.52	21.97	1750-1	M's; $\alpha'$ m; 12Hvw	1550-5	M'vs; $\alpha'$ m; 21Rw; $\beta\text{vw}$
21*	43.75	29.73	6.53	19.99	1750-1	M's; $\alpha'$ m; 21Rw	1550-5	M'vs; $\alpha'$ m
22*	36.96	9.60	23.88	29.56	1600-1	$\beta_{20}\text{s}$ ; 15Rm	1350-24	Avs; $\beta_{20}\text{m}$ ; 15Rvw
23*	28.04	17.81	42.61	11.54	1600-1	$\beta_{50}\text{vs}$ ; 15Rm; 12Hvw	1150-24 1350-24^	$\beta_{50}\text{vs}$ ; Us; 15Rm $\beta_{50}\text{s}$ ; As; 15Rm; MPm
24*	26.55	4.91	22.39	46.15	1550-1	M'w 12Hvw	1350-24	Avs; $\beta_{35}\text{W}$
25*	14.06	38.89	11.91	35.14	1750-1	M'vs; Am; AlNw; Uvw		

^Used for establishing phase relationships; ~ containing some  $\beta'$  with smaller unit cell dimensions;  $\alpha = \alpha$ - $\text{Si}_3\text{N}_4$ ;  $\alpha' = \alpha$ -sialon;  $\beta = \beta$ - $\text{Si}_3\text{N}_4$ ;  $\beta'$ ,  $\beta_6, \beta_{15}, \dots = \beta$ -sialon; A =  $\text{LnAlO}_3$ ; N =  $\text{Ln}_2\text{AlO}_3\text{N}$ ; MP =  $\text{LnAl}_{12}\text{O}_{18}\text{N}$ ; M' =  $\text{Ln}_2\text{Si}_{3-x}\text{Al}_x\text{O}_{3+x}\text{N}_{4-x}$ ; J =  $\text{Ln}_4\text{Si}_2\text{O}_7\text{N}_2$ ; H =  $\text{Ln}_{10}(\text{SiO}_4)_6\text{N}_2$ ; U =  $\text{Ln}_3\text{Si}_3\text{Al}_3\text{O}_{12}\text{N}_2$  (all Ln here represents Nd).

**Table 2.** Compositions studied in the system  $\text{Si}_3\text{N}_4\text{-AlN-Al}_2\text{O}_3\text{-Sm}_2\text{O}_3$ 

No.	$\text{Si}_3\text{N}_4$	Compositions (wt%)			Firing (°C-h)	Phases present	Heat treat.	Phases present
		AlN	$\text{Al}_2\text{O}_3$	$\text{Sm}_2\text{O}_3$				
1*	80.00	—	4.52	15.48	1700-1	$\beta$ vs; M'vw	1350-24	$\beta$ s; Hm
2*	75.77	1.06	1.81	21.36	1700-1	M'vs; $\beta$ s; $\alpha$ vw	1550-5 <sup>^</sup>	$\beta$ vs; M'w
3*	70.64	7.07	7.97	14.32	1700-1	$\beta_6$ s; $\alpha$ 'm; M'w	1550-5	M'vs; $\beta$ s
							1350-24	$\beta_6$ s; As; $\alpha$ 'w; M'w
4*	59.38	16.69	1.49	22.44	1750-1	M's; $\alpha$ 'm; $\beta$ 'vw	1550-5 <sup>^</sup>	$\beta_6$ vs; M's; $\alpha$ 'vw
5*	57.08	10.56	18.05	14.31	1700-1	$\beta_{13}$ s; $\alpha$ 'w; 12Hvw	1550-5	M's; $\alpha$ 'm; 21Rvw
							1350-24 <sup>^</sup>	$\beta_{13}$ s; As
							1550-5	$\beta_{13}$ vs; 12Hw
6*	43.46	29.66	6.49	20.39	1750-1	M's; $\alpha$ 'm; 21Rw	1550-5	M's; $\alpha$ 'm; 21Rw
7*	36.57	9.50	23.63	30.30	1550-3	$\beta_{20}$ s; 15Rm	1150-24	Uvs; $\beta_{20}$ m; 15Rm; SmSiO <sub>3</sub> ?
							1350-24 <sup>^</sup>	Avs; $\beta_{20}$ m
8*	28.05	17.81	42.51	11.63	1600-1	$\beta_{50}$ vs; 15Rm	1150-24	$\beta_{50}$ vs; Us; 15Rm
							1350-24 <sup>^</sup>	Avs; $\beta_{50}$ S~; MPm; 15Rw
9*	26.56	4.91	22.01	46.53	1600-1	$\beta_{20}$ s; 15Rm	1150-24	Uvs; $\beta_{20}$ m; 15Rm; SmSiO <sub>3</sub> ?
							1350-24 <sup>^</sup>	Avs; $\beta_{20}$ m; Uvw
10*	13.91	38.89	11.91	35.29	1750-1	M'vs; As; AlNw; 27Rvw		
11*	11.82	—	—	88.18	1650-1	Jvs		
12*	9.46	—	2.55	87.99	1650-1	Jvs		
13*	4.73	6.31	—	88.96	1550-1	Avs; Js; Sm <sub>2</sub> O <sub>3</sub> w		
14*	4.73	—	13.57	81.70	1550-1	Avs; Js; Sm <sub>2</sub> O <sub>3</sub> w		
15#	10.58	37.44	42.98	9.00	HP1750-1	15Rvs; MPw		
16#	9.17	41.00	40.84	8.99	HP1750-1	12Hvs; MPw; Aw		
17#	3.55	4.21	6.79	85.45	1600-2	Ns; Jm		

All the symbols have the same meaning as in Table 1 except Ln (here Ln represents Sm).

(99.9%, Yaolung Chemical Works, China<sup>#</sup> and 99.9%, Aldrick Chemical Co. Ltd<sup>\*</sup>). The oxygen contents of the nitride powders were taken into account in calculating the compositions. The starting powders were weighed out and ground in absolute alcohol<sup>#</sup> or isopropanol<sup>\*</sup> using an agate pestle and mortar. The mixed powders were dried and pressed into pellets 10 mm in diameter and were then isostatically pressed under a pressure of 200 MPa. The specimens prepared at Shanghai were fired in a graphite-resistant furnace with a rather slow cooling rate (~50°C/min) whilst those at Newcastle were fired in graphite-resistant or tungsten element furnaces both of which could be cooled down to room temperature very quickly (~100°C/min). A nitrogen atmosphere was used in all cases. The specimens with the compositions near liquid phase region were prepared in Shanghai and then heat-treated in Newcastle. The heat-treatment was carried out either in a tungsten element furnace (at 1150-1450°C) or in a molybdenum element furnace (at 1550°C). All specimens were examined by X-ray diffractometry<sup>#</sup> or using a Hägg-Guinier focusing camera<sup>\*</sup>. Only specimens showing less than 3% weight loss after firing were used for data analysis.

### 3 Results

Twenty five Nd-containing compositions and 17 Sm-containing compositions in the region

bounded by  $\text{Si}_3\text{N}_4$ , AlN,  $\text{Al}_2\text{O}_3$  and  $\text{Ln}_2\text{O}_3$  were studied to establish compatibility relationships. The binary tie lines established were based on the results listed in Tables 1 and 2. In the region explored, the same phases were observed in both systems, but it was noted that melting temperatures were lower in the samarium system and consequently, at a given temperature, the size of the

**Table 3.** Subsolidus compatibility tetrahedra in the systems  $\text{Si}_3\text{N}_4\text{-AlN-Al}_2\text{O}_3\text{-Ln}_2\text{O}_3$  (R = Nd and Sm)

$\text{Al}_2\text{O}_3\text{-}\beta_{60}\text{-15R-MP}$	$\text{Al}_2\text{O}_3\text{-15R-15R'-MP}$
$\text{Al}_2\text{O}_3\text{-15R'-12H'-MP}$	$\text{Al}_2\text{O}_3\text{-12H'-21R'-MP}$
$\text{Al}_2\text{O}_3\text{-21R'-AlN-MP}$	$\text{15R-15R'-12H-12H'-MP}$
$\text{12H-12H'-21R-21R'-MP}$	$\text{21R-21R'-27R-27R'-MP}$
$\text{27R-27R'-2H}^\delta\text{-2H}^\delta\text{-MP}$	$\text{2H}^\delta\text{-2H}^\delta\text{-AlN-MP}$
$\text{21R'-27R'-AlN-MP}$	$\text{27R'-2H}^\delta\text{-AlN-MP}$
$\text{AlN-2H}^\delta\text{-MP-LnAlO}_3$	$\text{2H}^\delta\text{-27R-MP-LnAlO}_3$
$\text{27R-21R-MP-LnAlO}_3$	$\text{21R-12H-MP-LnAlO}_3$
$\text{12H-15R-MP-LnAlO}_3$	$\beta_{60}\text{-15R-MP-LnAlO}_3$
$\beta_{60}\text{-Al}_2\text{O}_3\text{-MP-LnAlO}_3$	$\beta_{60}\text{-}\beta_{25}\text{-15R-LnAlO}_3$
$\beta_{25}\text{-15R-12H-LnAlO}_3$	$\beta_{25}\text{-}\beta_{10}\text{-12H-LnAlO}_3$
$\beta_{10}\text{-12H-LnAlO}_3\text{-M'}$	$\beta_{10}\text{-12H-21R-M'}$
$\alpha'\text{-}\beta_0\text{-}\beta_{10}\text{-M'}$	$\alpha'\text{-}\beta_{10}\text{-21R-M'}$
$\alpha'\text{-}\beta_{10}\text{-}\beta_8\text{-21R}$	$\alpha'\text{-}\beta_8\text{-21R-27R}$
$\alpha'\text{-}\beta_8\text{-}\beta_5\text{-27R}$	$\alpha'\text{-}\beta_5\text{-27R-2H}^\delta$
$\alpha'\text{-}\beta_5\text{-}\beta_2\text{-2H}^\delta$	$\alpha'\text{-}\beta_2\text{-2H}^\delta\text{-AlN}$
$\alpha'\text{-}\beta_2\text{-}\beta_0\text{-AlN}$	$\alpha'\text{-AlN-2H}^\delta\text{-M'}$
$\alpha'\text{-2H}^\delta\text{-27R-M'}$	$\alpha'\text{-27R-21R-M'}$
$\text{M'-12H-21R-LnAlO}_3$	$\text{M'-21R-27R-LnAlO}_3$
$\text{M'-27R-2H}^\delta\text{-LnAlO}_3$	$\text{M'-2H}^\delta\text{-AlN-LnAlO}_3$
$\text{M'-AlN-LnAlO}_3\text{-J}$	$\text{M'-AlN-J-M}$
$\text{AlN-LnAlO}_3\text{-J-Ln}_2\text{AlO}_3\text{N}$	$\text{LnAlO}_3\text{-J-Ln}_2\text{AlO}_3\text{N-Ln}_2\text{O}_3$

MP =  $\text{LnAl}_2\text{O}_7$ ; M' =  $\text{Ln}_2\text{Si}_3\text{N}_8\text{-Al}_2\text{O}_3\text{-N}_{4-x}$ ; J =  $\text{Ln}_4\text{Si}_2\text{O}_7\text{N}_2$ ; 15R, 12H, 21R, 27R, 2H<sup>δ</sup> are those on the Si-rich end of AlN polytypoids; 15R', 12H', 21R', 27R', 2H<sup>δ</sup> are AlN polytypoids on the Al-rich end.

liquid-forming region is larger. Based on the much more extensive knowledge of phase relationships in the Y-Si-Al-O-N system<sup>10-13</sup> and other information in the literature listed above, 44 compatibility tetrahedra were established in this region for both Nd and Sm (Table 3).

As indicated in this table, tie lines exist between the compound  $\text{LnAl}_{12}\text{O}_{18}\text{N}$  and all the AlN polytypoid phases as well as  $\beta_{60}$  (the maximum limit of the  $\beta$ -sialon solid solution). The compound  $\text{LnAlO}_3$  was found to be compatible with  $\beta$ -sialon in the range  $\beta_{10}(z = 0.8)$ – $\beta_{60}$ , and also with the

Si-rich terminal compositions of the AlN polytypoid phases. Compatibility tetrahedra are also formed between  $\alpha$ -sialon, the Si-rich ends of the AlN polytypoid ranges (from AlN to 21R) and M'-phase. M' was also found to have tie lines with  $\beta$ -sialon from  $\beta_0(\beta\text{-Si}_3\text{N}_4)$  to  $\beta_{10}$ , forming two  $\alpha' + \beta'$  containing compatibility tetrahedra  $\alpha' - \beta_0 - \beta_{10} - \text{M}'$  and  $\alpha' - \beta_{10} - 21\text{R} - \text{M}'$ .  $\text{LnAlO}_3$ –AlN polytypoid and  $\alpha' - \beta'$  two-phase regions are represented graphically in Figs 2–4. In the present work,  $\alpha$ -sialon is considered as a point composition and its detailed solid solution range has not been determined.

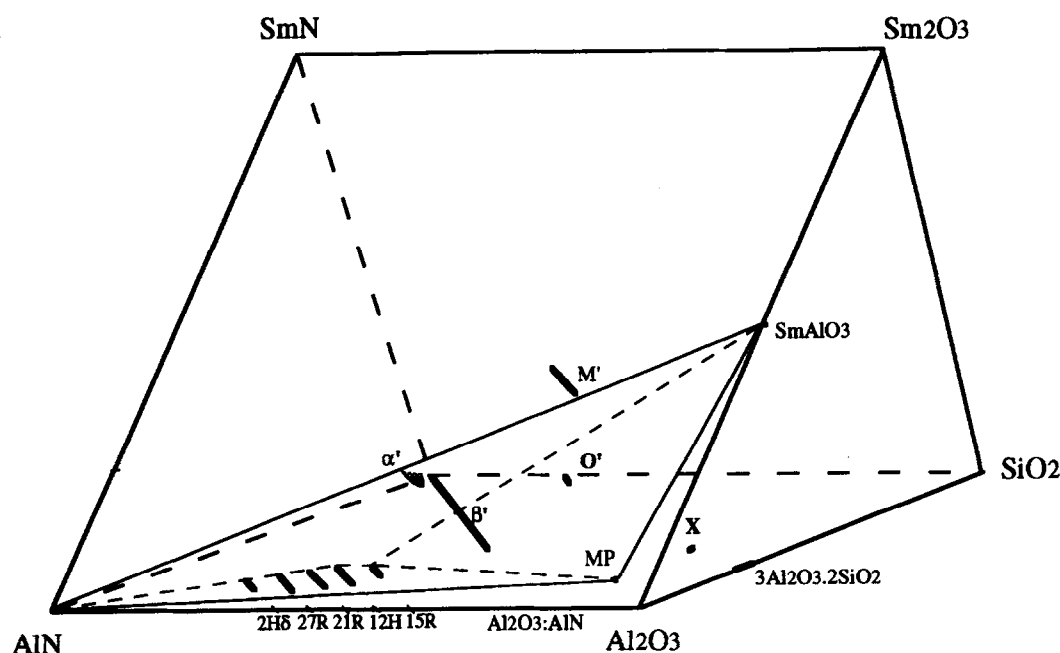


Fig. 2.  $\text{Sm}(\text{Nd})\text{AlO}_3$  is compatible with all polytypoid phases (Si-rich terminal), AlN and  $\text{Sm}(\text{Nd})\text{Al}_{12}\text{O}_{18}\text{N}$  (MP-compounds) forming five compatibility tetrahedra:  $\text{Sm}(\text{Nd})\text{AlO}_3$ –15R–MP–12H;  $\text{Sm}(\text{Nd})\text{AlO}_3$ –12H–MP–21R;  $\text{Sm}(\text{Nd})\text{AlO}_3$ –21R–MP–27R;  $\text{Sm}(\text{Nd})\text{AlO}_3$ –27R–MP–2H $\delta$  and  $\text{Sm}(\text{Nd})\text{AlO}_3$ –2H $\delta$ –MP–AlN.

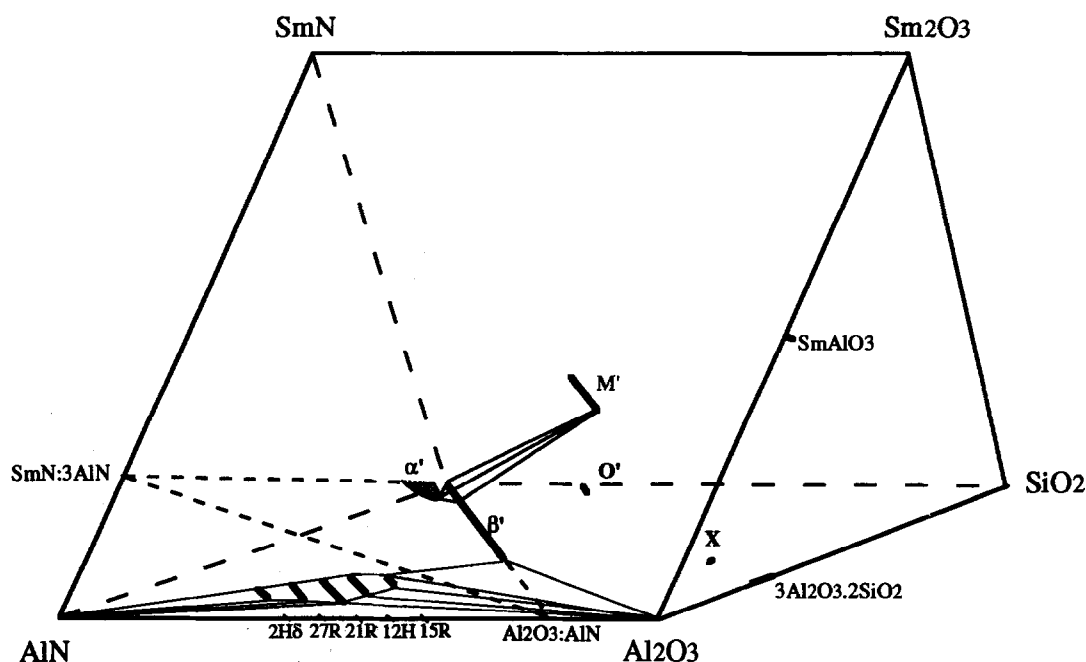
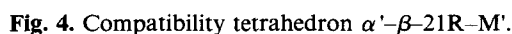
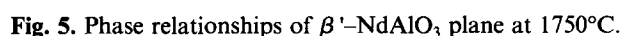


Fig. 3. M' (melilite solid solution) is compatible with  $\beta$ -sialon ( $\beta_0$ – $\beta_{10}$ ) and  $\alpha$ -sialon forming  $\alpha' - \beta' - \text{M}'$  compatibility tetrahedron.



Previous work in the Nd-system<sup>4</sup> showed that at 1700°C, the liquid phase region in this system intersects the  $\beta$ -sialon–NdAlO<sub>3</sub> plane (Fig. 5). Moreover, NdAlO<sub>3</sub> does not appear in nitrogen-rich compositions on this plane. These observations are in contrast to the behaviour of YAG (Y<sub>3</sub>Al<sub>5</sub>O<sub>12</sub>) in the  $\beta$ -sialon–YAG system. The appearance of 12H polytypoid phase on the  $\beta$ -sialon–NdAlO<sub>3</sub> plane implies that it must be in equilibrium with a liquid phase of more silica-rich

composition than those on the plane. Recently, heat-treatment studies of Ln-Si-Al-O-N (Ln = La-Yb) glasses,<sup>14</sup> have indicated that the resulting crystalline phases vary with the composition of the glass, the atomic number (i.e. ionic radius) of the rare earth element and with the heat-treatment temperature. In the Nd- and Sm-systems, at lower temperatures (1000–1200°C), wollastonite (LnSiO<sub>2</sub>N) and U-phase are the main crystalline phases formed from glasses in equilibrium with mixed  $\alpha + \beta$  sialons, and with increasing temperature, LnAlO<sub>3</sub> appears. U-phase, of composition



$\text{Ln}_3\text{Si}_{3-x}\text{Al}_{3+x}\text{O}_{12+x}\text{N}_{2-x}$ , where  $0 < x < 1$ , is a crystallization product of Ln–Si–Al–O–N glasses in equilibrium with  $\beta$ -sialon, heated in the range 950–1400°C. The stability of this phase increases with cation size, and the melting point is around 1390°C.<sup>6</sup>

In the region studied,  $\text{LnAlO}_3$ , M'-phase and U-phase were the main phases observed after heat-treatment in the temperature range 1150–1550°C. Suitable devitrification temperatures for the formation of  $\text{LnAlO}_3$  are in the range 1250–1450°C. At lower temperatures (1150–1250°C), U-phase occurred instead. In the oxygen-rich compositions explored in the present work, U-phase always occurred after heat-treatment (or even after firing in the Shanghai furnace, which has a slower cooling rate). The occurrence of U-phase in the region studied can not be considered as an equilibrium phase under subsolidus temperature conditions and is only an incompletely recrystallized form of the liquid phase. In  $\text{Si}_3\text{N}_4$ -rich compositions, M'-phase often occurs after sintering, increasing in amount after further heat-treatment at  $\approx 1550^\circ\text{C}$ . This is because the composition of M' is nearer to the liquid phase region and therefore M' phase dissolves into the melt during firing. The crystallization temperature for M' is about 1550°C. In establishing subsolidus phase relationships, the judgement on the correct equilibrium phases under subsolidus temperature conditions can sometimes be a difficult problem. Using phase assemblages observed at the same temperature for all conditions studied might lead to mistaken results, since different compositions may need different temperatures to fully crystallize the liquid phase.

In the present work, all starting compositions were designed to fall on supposed tie lines or into supposed compatibility triangles. For examples, in the Sm system, compositions Nos 2, 3 and 5 were on the lines between M' ( $\text{Ln}_2\text{Si}_2\text{AlO}_4\text{N}_3$ ) and  $\beta\text{-Si}_3\text{N}_4$ ,  $\beta$ -sialon ( $z = 1$ ) and  $\beta$ -sialon ( $z = 2$ ) respectively; Nos 1, 8 and 9 were on composition lines between  $\text{SmAlO}_3$  and  $\text{Si}_3\text{N}_4$ ,  $\beta$ -sialon ( $z = 4$ ) and  $\beta$ -sialon ( $z = 2$ ), respectively. If the expected phases were obtained after heat-treatment under a particular set of conditions, then equilibrium was believed to have been achieved. Based on this philosophy, compositions marked with the symbol '^' in Tables 1 and 2 were believed to have achieved equilibrium and were used to establish the subsolidus phase relationships. Composition No. 1 (Table 2) only gave M' and apatite ( $\text{Sm}_{10}(\text{SiO}_4)_6\text{N}_2$ ) after heat treatment at 1350 and 1550°C, which indicated that the supposed tie line  $\beta\text{-Si}_3\text{N}_4\text{--SmAlO}_3$  does not exist. In composition No. 5 (Table 2), the absence of M' phase implies that M' is not compatible with  $\beta_{13}$ . The coexis-

tence of  $\beta$ -sialon with M' was found to be restricted to the range  $\beta_0\text{--}\beta_{10}$ . From the X-ray diffraction data of M' and  $\beta$ -sialon, it seems that Nd- and Sm-melilite ( $\text{Ln}_2\text{O}_3\cdot\text{Si}_3\text{N}_4$ ) has priority over  $\beta\text{-Si}_3\text{N}_4$  in accommodating Al and O (thereby forming M' phase) and therefore the tie lines between melilite and  $\beta$ -sialon do not run parallel. The oxygen-containing  $\alpha$ -sialon phase occurring in the present samples is believed to have a composition close to the oxygen-rich limit of the  $\alpha$ -sialon homogeneity range in these systems; this phase is also compatible with M'.

$\alpha$ -sialon, 12H and 15R sometimes occurred in compositions located on the  $\beta$ -sialon– $\text{LnAlO}_3$  and  $\beta$ -sialon–M' planes, and decreased in amount or even disappeared after heat-treatment. This is partly because the liquid phase in these compositions shifts in composition with temperature, and also because some  $\alpha \rightarrow \beta$  sialon transformation occurs in these samples.<sup>15</sup> J-phase ( $\text{Ln}_4\text{Si}_2\text{O}_7\text{N}_2$ ) should occur in compositions along the line joining  $\text{Ln}_2\text{O}_3$  to  $\text{Si}_2\text{N}_2\text{O}$ , but it always appears at the composition  $3\text{Ln}_2\text{O}_3\cdot\text{Si}_3\text{N}_4$ , just as in the Y–Si–Al–O–N system. This could be attributed to the unavoidable existence of a silica layer on the surface of silicon nitride. In the Y–Si–Al–O–N system, J-phase forms a continuous solid solution with YAM ( $\text{Y}_4\text{Al}_2\text{O}_9$ ). In the present work J-phase solid solution (J') was never observed. Composition Nos 11 and 12 (Table 2) were designed to produce J- and J'-phase and the X-ray data did not show visible differences in d-values between these two J-phases.

Of the 44 compatibility tetrahedra established in the present work, the following six which involve  $\alpha$ -,  $\beta$ -sialon and AlN-polytypoids (which could be used as reinforcement phase for  $\alpha'$ ,  $\beta'$  or  $\alpha'\text{--}\beta'$  because of its fibre-like morphology) and the promising grain boundary phases M' and  $\text{LnAlO}_3$ , are the most useful for the design of multi-phase sialon ceramics. They are:  $\alpha\text{-sialon--}\beta_0\text{--}\beta_{10}\text{--M'}$ ;  $\alpha\text{-sialon--}\beta_{10}\text{--21R--M'}$ ;  $\beta_{25}\text{--15R--12H--LnAlO}_3$ ;  $\beta_{25}\text{--}\beta_{10}\text{--12H--LnAlO}_3$ ;  $\beta_{10}\text{--12H--LnAlO}_3\text{--M'}$  and  $\beta_{10}\text{--12H--21R--M'}$ .

## 5 Conclusions

Subsolidus phase relationships in the systems  $\text{Ln}_2\text{O}_3\text{--Si}_3\text{N}_4\text{--AlN--Al}_2\text{O}_3$  (Ln = Nd, Sm) have been determined. Forty-four compatibility tetrahedra have been established in this region.  $\text{LnAlO}_3$  coexists with  $\beta$ -sialon, approximately from  $\beta_{10}$  ( $z = 0.8$ ) to  $\beta_{60}$  ( $z = 4$ ). The liquid phase crosses the tie line between  $\text{LnAlO}_3$  and  $\beta$ -sialon at firing temperatures (1600–1700°C) and therefore  $\beta$ -sialon– $\text{LnAlO}_3$  two-phase materials can only be

obtained after heat-treatment in the range 1250–1450°C. The coexistence of M' with  $\beta$ -sialon is restricted to the range  $\beta_0$ – $\beta_{10}$ .  $\alpha$ -Sialon is also compatible with M'. The compatibility tetrahedra  $\alpha$ -sialon– $\beta_0$ – $\beta_{10}$ –M';  $\alpha$ -sialon– $\beta_{10}$ –21R–M';  $\beta_{25}$ –15R–12H–LnAlO<sub>3</sub>;  $\beta_{25}$ – $\beta_{10}$ –12H–LnAlO<sub>3</sub>;  $\beta_{10}$ –12H–LnAlO<sub>3</sub>–M' and  $\beta_{10}$ –12H–21R–M' are the most useful for the design and processing of multi-phase sialon ceramic materials.

## Acknowledgement

This work was supported by NNSF (National Natural Science Foundation, China) and the ALCS (Academic Link with China Scheme) programme of the British Council, UK.

## References

1. Mitomo, M., Izumi, F., Horiuchi, S. & Matsui, Y., Phase relationships in the system Si<sub>3</sub>N<sub>4</sub>–SiO<sub>2</sub>–La<sub>2</sub>O<sub>3</sub>. *J. Mater. Sci.*, **17** 1982 2359–66.
2. Sun, W. Y., Yen, T. S. & Tien, T. Y., Subsolidus phase relationships in the system Re–Al–O–N (where R = rare earth elements). *J. Solid State Chem.*, **95** 1991 424–9.
3. Huang, Z. K., Tien, T. Y. & Yan, D. S., Subsolidus phase relationships in Si<sub>3</sub>N<sub>4</sub>–AlN–rare earth oxide systems. *J. Amer. Ceram. Soc.*, **69** 1986 C241–2.
4. Slasor, S., Liddell, K. & Thompson, D. P., The role of Nd<sub>2</sub>O<sub>3</sub> as an additive in the formation of  $\alpha'$  and  $\beta$ -sialon. In *Proc. Special Ceramics* 8, ed. S. P. Howlett and D. Taylor, British Ceramics Society, UK, 1986, pp. 35–50.
5. Thompson, D. P., New grain boundary phases for Si<sub>3</sub>N<sub>4</sub> and sialon ceramics. In *Proc. C-MRS Int. Symp. ('90, Peking)* Vol 2., ed. Y. Ham, Elsevier Science BV, Amsterdam, 1991, pp. 335–42.
6. Mandal, H., Thompson, D. P. & Ekström, T., Heat-treatment of Ln–Si–Al–O–N glasses. In *Proc. 7th Irish Mater. Forum Conf. IMF7*, ed. M. Buggy and S. Hampshire. Trans. Tech. Publications, Switzerland, 1992, pp. 187–203.
7. Thompson, D. P., New grain-boundary phases for nitrogen ceramics. In *Mat. Res. Soc. Symp. Proc. Symposium K* Vol. 287, ed. I.-W. Chen *et al.*, MRS, 1993, pp. 79–92.
8. Cheng, Y.-B. & Thompson, D. P., Aluminium-containing nitrogen melilite phases. *J. Amer. Ceram. Soc.*, **77** (1994) 143–8.
9. Cheng, Y.-B. & Thompson, D. P., Preparation and grain-boundary devitrification of samarium  $\alpha$ -sialon ceramics. *J. Eur. Ceram. Soc.*, **14** (1994) 13–21.
10. Thompson, D. P., Phase relationships in Y–Si–Al–O–N ceramics. In *Proc. Int. Symp. Tailoring Multiphase and Composite Ceramics*, ed. R. E. Tressler *et al.* MRS Vol. 20, 1986, pp. 93–102.
11. Sun, W. Y., Tien, T. Y. & Yen, T. S. (Yan, D. S.), Solubility limits of  $\alpha'$ -SiAlON solid solutions in the system Si, Al, Y/N, O. *J. Amer. Ceram. Soc.*, **74** (1991) 2547–50.
12. Sun, W. Y., Tien, T. Y. & Yen, T. S. (Yan, D. S.), Subsolidus phase relationships in part of the system Si, Al, Y/N, O: the system Si<sub>3</sub>N<sub>4</sub>–AlN–YN–Al<sub>2</sub>O<sub>3</sub>–Y<sub>2</sub>O<sub>3</sub>. *J. Amer. Ceram. Soc.*, **74** (1991) 2753–8.
13. Sun, W. Y., Yen, T. S. & Tien, T. Y., Graphical representation of the sub-solidus phase relationships in the reciprocal salt system Si, Al, Y/N, O. *Sci. in China (Series A)*, **35** (1991) 877–89.
14. Mandal, H. & Thompson, D. P., Heat-treatment of sialon ceramics densified with higher atomic number rare earth and mixed yttrium/rare earth oxides. In *Proc. Special Ceramics* 9, ed. R. Stevens. The Institute of Ceramics, Stoke-on-Trent, UK, 1992, pp. 97–104.
15. Mandal, H., Thompson, D. P. and Ekström, T., Reversible  $\alpha \rightleftharpoons \beta$  sialon transformation in heat-treated sialon ceramics. *J. Eur. Ceram. Soc.*, **12** (1993) 421–9.